Advances in Thermal Processes
and Energy Transformation
Volume 5, 2022, DZUR01, p. 36-39, ISSN 2585-9102
https://doi.org/10.54570/atpet

Methods for Determining Thermal-mechanical Wear of Refractory Materials

Róbert Dzurňák[1] ● Gustáv Jablonsky[1] ● Augustín Varga[1]● Šimon Staško[1]● Gabriel Sučik[2]● Beatrice Plesingerová[2]● Radka Bakajsová[2]

[1]Department of Thermal Engineering and Gas Industry, Faculty of Materials, Metallurgy and Recycling, Institute of Metallurgy, Technical University of Košice, Letná 9, 042 00 Košice, Slovak Republic, robert.dzurnak@tuke.sk, gustav.jablonsky@tuke.sk
[2]Department of Non-ferrous Material, Faculty of Materials, Metallurgy and Recycling, Institute of Metallurgy, Technical University of Košice, Letná 9, 042 00 Košice, Slovak Republic, gabriel.sucik@tuke.sk, beatrice.plesingerova@tuke.sk

Category : Review Article
Received : 12 October 2022 / Revised: 26 October 2022 / Accepted: 30 October 2022

Keywords : corrosion, refractory material, testing

Abstract : The presented article deals with methods of testing refractory materials that are currently most often used for testing low-temperature corrosion caused by biomass ash. The article deals with the effect of the chemical composition of biomass on melting temperatures and what standards are used to evaluate these processes. The article also discusses the methods of testing the abrasion of the surfaces of refractory materials. The article points out that at the same time the testing methods are not sufficient for evaluation and that the testing conditions do not reflect the operating parameters achieved in real devices.

Citation: Dzurňák Róbert, Jablonský Gustáv, Varga Augustín, Staško Šimon, Sučik Gabriel, Plesingerová Beatrice, Bakajsová Radka: Methods for Determining Thermal-mechanical Wear of Refractory Materials, Advance in Thermal Processes and Energy Transformation, Volume 5, No. 3, (2022), p. 36-369, ISSN 2585-9102. https://doi.org/10.54570/atpet

1 Introduction

In the current era, which is associated with several crises, whether it is an ecological crisis, an energy crisis or the war in Ukraine, there is a constant challenge to bring new ways of using renewable energy sources. These resources can locally help reduce the impact of the above-mentioned crises on the national economy and thus also bring sustainable development of environmental protection. The current trend of reducing the carbon footprint of technological processes causes certain types of renewable resources to be used in processes in which they did not appear in the past, which results in many advantages but also related disadvantages of the given application. Among such applications when an alternative source of energy is used as a replacement for classic fossil fuels, it is possible to include e.g. the use of biomass in the metallurgical process, in the energy sector and the like. Current knowledge about the usability of biomass in the metallurgical industry was defined in publications in the processing of ferrous materials [1,2,3], in the combined production of electricity and heat in the framework of co-combustion of biomass [4,5,6,7].

All the above-mentioned applications involve the thermochemical decomposition of biomass, after which the solid residue - ash is formed. Biomass ash is composed of several components. The determination of the ash content methodology in solid biofuels is determined by the STN EN ISO 18122 standard. A detailed analysis of the chemical composition of ash from biomass was prepared by Vassilev [8], where he compared several forms of biomass in terms of the percentage share of individual ash components. The most frequently occurring elements in biomass ash are SiO_2, CaO, K_2O, P_2O_5, Al_2O_3, MgO, Fe_2O_3, SO_3, Na_2O, TiO_2 [8]. The interaction of biomass ash most often affects the heat exchange surfaces near the combustion zone, which are formed by lining in thermal aggregates.

Low-temperature corrosion occurs on these surfaces, which is caused by the low melting temperature of the ash. Abrasion of the surface of the heat exchange surfaces can also be caused by ash. The above-mentioned influences have a significant impact on the service life of linings, and therefore it is important to analyze the influence of the chemical composition of biomass on heat exchange surfaces.

The aim of the presented article is to create an overview of the current knowledge about the influence of biomass ash on the wear of refractory materials and to describe the methods of their testing at the present time.

2 The influence of the chemical composition of biomass on ash melting

The main elements influencing the properties of ash contained in wood are calcium, magnesium, silicon and potassium. Above all, the concentration of calcium, magnesium, potassium, but also sodium in the ash affects its fusibility. While calcium and magnesium increase the ash melting temperature, potassium and sodium decrease it [9]. The low melting point of ash leads to its sintering and the formation of slag and deposits in the incinerator. Silicon in the form of potassium silicate also affects the fusibility of ash by lowering the melting temperature. Phosphorus, richly contained in biofuels from phytomass, is partially volatile and can also cause a decrease in the ash melting temperature by forming phosphates. The main element creating aerosols during combustion is potassium. Its high concentration accelerates the formation of aerosols during combustion, which increases not only the emissions of solid pollutants, but also the clogging of the boiler. Sodium also exhibits similar properties during combustion. Problems related to ash fusibility increase with the application of biofuel produced from phytomass due to its relatively high potassium concentrations. The STN EN ISO 21404 standard determines the methodology for determining the melting temperature of biomass ash. A mathematical model that defines the basic degree of fusibility according to the standard based on the chemical composition of the ash was proposed by Holubčik [9]. The lower limit of fusibility of ash from biomass is from about 915°C for straw. For other types of biomass, the melting range of ash is from 1100°C to 1400°C.

3 Methods of testing corrosion of linings

Currently, various methods of testing linings are used. The main purpose is to test the effect of slag (from biomass ash) on the surface of refractory material. The guideline for determining the corrosion of refractory materials by the action of melts is defined by the European directive P CEN/TS 15418. Testing can be divided into 2 main groups based on the conditions under which the test is performed. Static testing is one in which there is no mixing of the refractory material from the slag. In this case, the corrosion wear of the refractory material is smaller compared to the operating conditions in the furnace, but they allow studying the chemical reactions between the lining and the slag. The most commonly used static tests include crucible tests or immersion tests.

The basis of the crucible test (Fig. 1) is a lining in which a hole of certain dimensions is created. The shape of the lining is usually a cylinder or cuboid with a wall 100 mm long. The diameter of the hole is 55 mm and the depth of the hole is 55 mm. A corrosive material is placed in the hole and at a temperature above 1450°C in an electric furnace; the corrosive material is allowed to react with the walls of the analysed lining for several hours. [10,11] dealt with the effect of corrosion of the masonry due to biomass slag in their works. Within the electric furnace, it is possible to place several analysed samples at the same time; therefore this evaluation method is used most often.

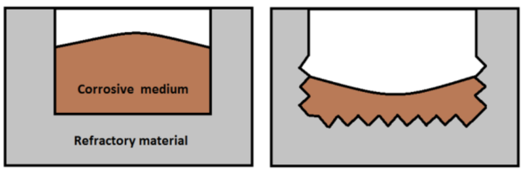

Figure 1 Crucible test

Another way to test refractory materials is to immerse the refractory material in the form of a rod or prism into a corrosive material. The dimensions of the analysed material are 10-30 mm in diameter and 50-120 mm in length. The basis of the method is an induction crucible furnace in which the corrosive material is melted. Rods made of refractory material are immersed 50 to 70 % in a corrosive environment. Degradation of the walls is subsequently evaluated through the loss of weight of the refractory material [12].

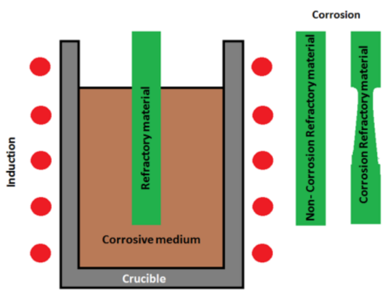

Figure 2 Immersion test

Another group of methods that are used to evaluate the corrosion of refractory materials are dynamic tests.

In dynamic tests, the melt (slag) from the biomass is mixed with the refractory material, thereby intensifying the corrosion process. The advantage of dynamic tests is to get closer to real operating conditions. On the other hand, however, they are more difficult to implement. The simplest type of dynamic test is the application of an immersion test, with the refractory rotating around a vertical axis.

A dynamic test in which the heat source is convective combustion of fuel and corrosive material is applied to the surface of the masonry is called a rotary slag test. As part of this test, a rotating drum is used, on one side of which a burner is placed, and on the opposite side, a solid corrosive material is injected onto the tested lining. Due to the heat from the flame, the corrosive material melts and interacts with the surface of the refractory material. The speed of rotation of the drum is 2 to 6 revolutions per minute. The heat source is most often propane burned with oxygen [13].

4 Methods of testing the abrasion of linings

In addition to the corrosion of the refractory material, the abrasion resistance of the material is also an important factor in the evaluation. Abrasion is damage to materials when they come into contact with a foreign body, which results in loss of material or grinding. Abrasion resistance is defined by the ASTM C704 standard for refractory materials. The testing conditions according to this standard are ambient temperature (20°C), air pressure 440kPa, amount of abrasive material used 1000g. SiC is used as an abrasive material. Particle size is graded.

The physical properties of refractory materials change under the influence of temperature, therefore the ASTM C704 standard does not take into account real operating conditions in this case. There are ways in the world to test refractory materials at higher temperatures. The Chinese researchers' device design was compared with British and Japanese standards in an article by Yonggang[14]. On the basis of the given article, it is possible to test brickwork up to a temperature of 1400°C. Yonggangg's test equipment design was to place a 114mm x 114mm or 100mm x 100mm refractory under test in a vertical ceramic tube. The source of heat was electric heating. The pressure conditions of the compressed air used to transport the abrasive material and the amount of the abrasive material were in accordance with the ASTM C704 standard.

5 Discussion

The above-mentioned methods of testing refractory materials are operated under artificially created conditions that do not reflect real conditions in combustion plants. The methods lack the distribution of ash particles in the working space and the way they create an adhesive on the linings. Some of the given effects can be tested using the dynamic method of the rotary slag test, but the disadvantage of this test is the counter-current movement of ash to the flue gas, which means that the ash moves from areas of lower temperatures to areas of high temperatures. However, in real conditions when co-burning biomass or replacing fossil fuel with biomass, the movement of ash is co-current. The proposal of a new testing method should be a dynamic analysis of corrosion testing, which would take into account the distribution of corrosive material in a co-current regime. In this way, it would also be possible to analyse the abrasion of the material at the working temperature of the heat aggregate. New methods of testing refractory materials will be introduced in the future.

6 Conclusion

Current corrosion testing methods or abrasion of the surfaces of refractory materials for operating under artificially created conditions that do not reflect real conditions in combustion plants. It is necessary to develop a new methodology for testing materials and analyse the results of its implementation in the framework of experimental measurements.

7 The reference list

[1] WEI, R.F., ZHANG, L.L., CANG, D.Q., LI, J.X., LI, X.W., XU, C.C.: Current status and potential of biomass utilization in ferrous metallurgical industry, *Renew. Sustain. Energy Rev.*, Vol. 68, pp. 511-524, 2017.

[2] MOUSA, E., WANG, C., RIESBECK, J., LARSSON, M.: Biomass applications in iron and steel industry: An overview of challenges and opportunities, *Renew. Sustain. Energy Rev.*, Vol. 65, pp. 1247-1266, 2016.

[3] LEGEMZA, J., FRÖHLICHOVÁ, M., FINDORÁK, R.: *Biomass and Carbon Fuels in Metallurgy*, 1st ed., Boca Raton, CRC Press, 2020.

[4] YANG, J., LI, Z., WEI, R., ZHOU, D., LONG, H., LI, J., XU, C.: Co-Combustion of Food Solid Wastes and Pulverized Coal for Blast Furnace Injection: Characteristics, Kinetics, and Superiority, *Sustainability*, Vol. 14, No. 12, p. 7156, 2022.

[5] VARINY, M., VARGA, A., RIMÁR, M., JANOŠOVSKÝ, J., KIZEK, J., LUKÁČ, L., JABLONSKÝ, G., MIERKA, O.: Advances in Biomass Co-Combustion with Fossil Fuels in the European Context: A Review, *Processes*, Vol. 9, No. 1, p.100, 2021.

[6] LUND, P.D., LINDGREN, J., MIKKOLA, J., SALPAKARI, J.: Review of energy system flexibility measures to enable high levels of variable renewable electricity, *Renew. Sustain. Energy Rev.*, Vol. 45, p. 785, 2015.

[7] SALOMÓN, M., SAVOLA, T., MARTIN, A., FOGELHOLM, C. J., FRANSSON, T.: Small-scale biomass CHP plants in Sweden and Finland, *Renew. Sustain. Energy Rev.*, Vol. 15, No. 9, pp. 4451-4465, 2011.

[8] VASSILEV, S. V., BAXTER, D., ANDERSEN, L. K., VASSILEVA, C. G.: An overview of the chemical composition of biomass, *Fuel*, Vol. 89, No. 5, pp. 913-933, 2010.

[9] HOLUBCIK, M., JANDACKA, J., MALCHO, M.: Ash melting temperature prediction from chemical composition of biomass ash. *The holistic approach to environment*, Vol. 5, No. 3, pp. 119-125, 2015.

[10] PLEŠINGEROVÁ, B., VADÁSZ, P., MEDVEĎ, D., SUČIK, G., MACHÁČEK, J., POPOVIČ, Ľ., BAKAJSOVÁ, R.: The effect of increasing MgO content in dendromass on ash fusibility and corrosion of corundum refractory castable, *Ceramics International*, Vol. 48, No. 15, pp.21739-21747, 2022.

[11] OVČAČÍKOVÁ, H., VELIČKA, M., VLČEK, J., TOPINKOVÁ, M., KLÁROVÁ, M., BURDA, J.: Corrosive Effect of Wood Ash Produced by Biomass Combustion on Refractory Materials in a Binary Al–Si System, *Materials*, Vol. 15, No. 16, p. 5796, 2022.

[12] Vlček, J., Ovčačíková, H., Klárová, M., Topinková, M., Burda, J., Velička, M., ... & Lang, K. (2019, November). Refractory materials for biomass combustion. In AIP Conference Proceedings (Vol. 2170, No. 1, p. 020024). AIP Publishing LLC. https://doi.org/10.1063/1.5132743

[13] VAINIO, E., KINNUNEN, H., LAURÉN, T., BRINK, A., YRJAS, P., DEMARTINI, N., HUPA, M.: Low-temperature corrosion in co-combustion of biomass and solid recovered fuels. *Fuel*, Vol. 184, pp. 957-965, 2016.

[14] LI, Yonggang: A New Test Method for Hot Abrasion Resistance on Refractories, *China's Refractories*, Vol. 20, No. 3, 2011.

Acknowledgement

This work was supported by the Slovak Research and Development Agency within the project APVV-17-0483 entitled "Ceramic materials for refractory lining of boilers with intensified combustion of biomass", and the Slovak Grant Agency through VEGA–No.1/0060/22 project entitled “Study of the impact of the binder phase composition on the corrosion of refractory materials in high-temperature reactors processing metal and waste “.

Advances in Thermal Processes and Energy Transformation
Volume 5, 2022, LUKA01, p. 40-44, ISSN 2585-9102
https://doi.org/10.54570/atpet

Heat Loss Reduction in the Selected Hot Water Distribution System

Peter Lukáč

Department of Power Engineering, Faculty of Mechanical Engineering, Technical University of Kosice, 042 00 Košice, Slovakia, peter.lukac@tuke.sk

Category : Original Scientific Paper
Received : 17 October 2022 / Revised: 26 October 2022 / Accepted: 27 October 2022

Keywords : Distribution system, hot water, heat loss, test measurements

Abstract : One possibility of reducing the energy consumption of buildings is to reduce heat loss in hot water distribution system kept in buildings. The aim of this paper is to present the results of research, which focused on energy efficiency of the distribution system of hot water in residential buildings. As part of the research have been carried out test measurements on the hot water distribution line and air temperature around the distribution line. Test measurements were conducted in two separate stages, in which measurements were made, as with continuous and intermittent operation in distribution system. The first stage of measurements took place before reconstruction of hot water distribution system when pipes weren´t insulated with thermal insulation. The second stage took place after reconstruction of the system, when pipes were fitted with thermal insulation. The aim of the research was to determine the course of the temperature of the water in the distribution system in different stages and highlight the effectiveness of isolating the hot water distribution system.

Citation: Lukáč Peter: Heat Loss Reduction in the Selected Hot Water Distribution System, Advance in Thermal Processes and Energy Transformation, Volume 5, No. 3, (2022), p. 40-44, ISSN 2585-9102. https://doi.org/10.54570/atpet

1 Introduction

A lost heat is indirectly used for the building heating in a winter season. However the heat from HW transferred through the pipe walls into building flats is the unwanted heat energy loss in a summer season. Properly designed HW distribution system can reduce the heat losses to the minimum [1].

According to the location of the pipe (inside or outside) and its position (horizontal or vertical), standard [2] states the relations for calculating the heat transfer coefficient.

Decree (3) deals with insulation for heat and hot water distribution. The optimal design of distribution systems cannot be done without thorough isolation of the pipe distribution, including devices and fittings, which must be included in every project documentation of heating and sanitary installations for construction implementation. The decree deals with insulation for heat and hot water distribution [3,4].

To obtain information on the course of the hot water temperature in the distribution system and the hot water circulation were carried out experimental measurements. Experimental measurements preceded by a theoretical analysis of the distribution system under consideration, from which it is clear that the greatest heat losses in the distribution system at 45 years of age unreconstructed residential buildings are from hot water risers and HW circulation. The transferred analysis shows that after using of thermal insulation for risers in an residential building can achieve savings of up to 52 % of heat loss.

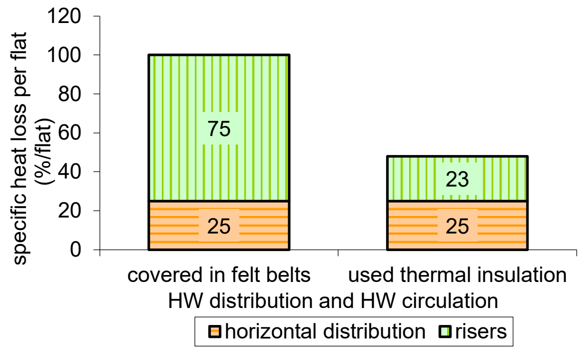

Figure 1 The specific heat loss of hot water distribution systems in residential building per flat - (% / flat)

Therefore, the subject of the test measurement was selected a hot water riser in residential building. The aim of the measurements is to detect how it changes the course of the hot water temperature in real conditions of use in the residential building.

2 The characteristics of the measured object

Residential building is located in a housing estate in Košice. From a structural point of view it is a prefabricated apartment building T 06 B, which is supplied with heat and hot water from a central heating system. Residential building consists of eight residential floors and one technical floor.

Hot water is fed into the building by underground duct in hot water channel from heat exchanger station. In the technical floor pipes of hot water and circulation stand out from the hot water channel under the ceiling of a technical floor and continues to each footboard. By risers is hot water distributed to individual flats. One hot water supply riser along 8 residential the cores located one above the other. In one of the residential core of the following plumbing fixtures are supplied with hot water: wash basin, bathtub and kitchen sink.

The measurement was carried out in the months of April to October. In the course of the test measurements in residential building was accomplished reconstruction of hot water riser, the HW circulation and cold water distribution. The measurement was carried out in continuous HW circulation and intermittent supply of HW or HW intermittent circulation.

2.1 Characteristics of distribution system before reconstruction

The original inlet hot water riser was made after full of steel threaded galvanized pipes DN32 lightness. Thermal conductivity of the steel tube is λ = 46.5 W.(m.K)$^{-1}$. The length of the hot water riser is 21.2 m. Hot water circulation piping was made over the height of the threaded galvanized steel pipe size DN20. The length of the riser is 21.2 m.

Hot water supply and circulation piping was before reconstruction covered in felt belts. Thermal conductivity of the felt belt is λ = 0.07 W.(m.K)$^{-1}$. Pipes covered in felt belts depending on design analysis can not be considered as effective thermal insulation.

It should be mentioned that the pipes of cold water was also covered in felt belts.

2.2 The characteristics of the distribution system after reconstruction

The new supply HW riser was made from the pipes of galvanized steel threaded DN32 and DN25. The riser DN32 is 12.7 meters long and DN25 is 8.4 meters long. Thermal conductivity of steel pipe is λ = 46.5 W.(m.K)$^{-1.}$

New circulating hot water piping is made after full building from plastic multilayer tubing PE-Al-PE with the outside diameter D 16 mm and wall thickness of the tube 2 mm. Pipe size is after calculation DN12. Thermal conductivity of plastic pipe is λ = 0.43 W.(m.K)$^{-1}$. All pipes are cover in PE insulation with thickness 10 mm. (λ = 0.04 W.(m.K)$^{-1}$.

3 The methodology of measurement and used measuring instruments

3.1 The methodology of the test measurements

The aim of the test measurement was an experimental monitoring of the actual temperature:

- temperature of the water in the pipe supplying water to the individual flats,
- temperature of the water circulation in the oven,
- air temperature in the installation shaft,
- air temperature in the room where there is a service shaft.

Test measurements were done separately for distribution hot water pipes before reconstruction, in particular to divorce after reconstruction. The measurements were conducted during continuous operating and intermittent operation of the distribution system. Interval recording of the measured temperatures was determined according to the severity of the ongoing processes in the distribution system. Interval temperature recording 3 minutes and 5 minutes were used for intermittent operation especially for cooling of hot water and measurement interval 30 minutes was used mainly in continuous operation.

3.2 The measuring instruments

For the test measurements were used temperature sensors with the recorder PMICRO-T. For pipes, where the temperature monitoring has been used contact PT1000 resistance temperature sensor that was installed on the cleaned pipe and then perfectly thermally insulated. Temperature sensor was connected to a recording device via a communication cable. For sensing the air temperature in the installation shaft was used sensor Microwire, which was suspended in space. Temperature sensor was connected to a recording device via a communication cable.

Measuring instruments at a set time interval measured temperature value and stored in its own memory.

Technical parameters of measuring instrument PMICRO-T:

Temperature range:	- 40°C to 125°C
Temperature resolution:	0.065°C
Maximum uncertainty:	0.5°C
Temperature sensor for water:	surface resistance PT100
Temperature sensor for air:	digital Microwire
Number of entries:	10400
The structure of the record:	day, month, year, hour, minute, temperature

Interval measurement:	1 to 255 minutes
Dimensions:	44 x 32 x 22 mm
Coverage:	IP 40
Transfer rate:	9200 bit /sec
PC connection:	RS232 COM port

3.3 Deployment of sensors

The placement of the temperature sensors is shown in Figure 2. The sensing of temperature sensors in the pipes were attached to the wall of the pipe and are provided with thermal insulation. Sensor sensing the air temperature in the area were suspended in space.

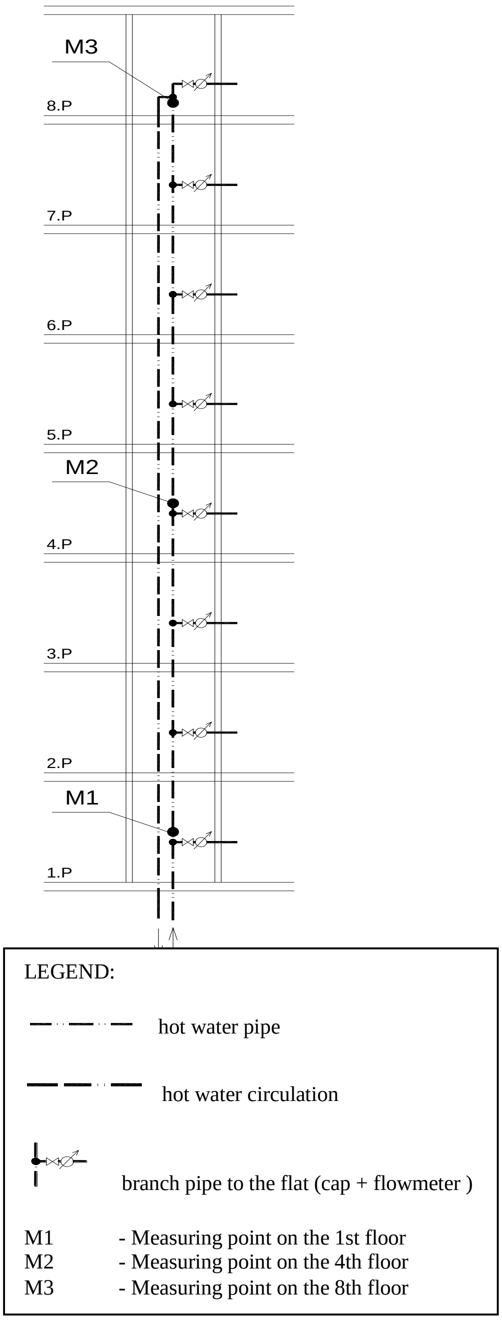

Figure 2 The placement of the temperature sensors

4 Test measurements of the distribution of hot water

Test measurements were conducted in two separate stages with continuous and intermittent operation of the distribution HW supply. The first stage took place before reconstruction of HW riser and second stage took place after reconstruction of HW distribution.

4.1 Test measurements with continuous operation of the HW distribution system before reconstruction distribution

The test measurement was carried out in May and April and was carried out with continuous operation of the distribution system. Recording interval of the measured temperatures was 30 minutes. In Figures 3 and 4 is processed week course of the measured temperatures of hot water and hot water circulation.

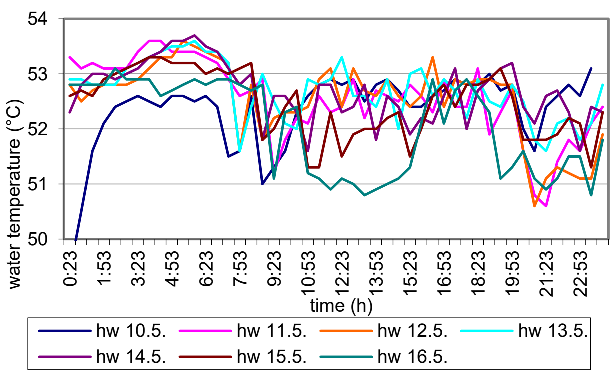

Figure 3 The course of the HW temperature in the pipes without insulation

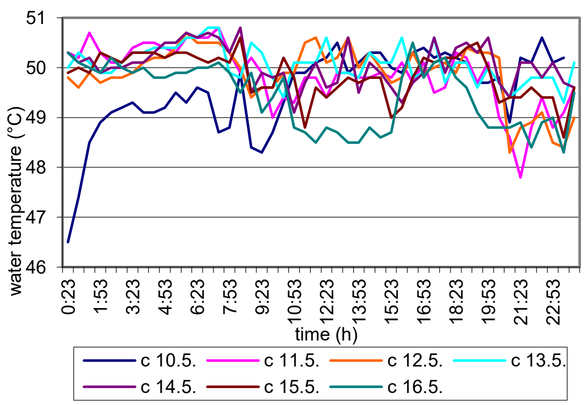

Figure 4 The course of the HW temperature in the circulation pipes without insulation

As is evident from Figures 3 and 4 in the pipes without insulation temperature for the day is uneven. In the HW pipe temperature values are recorded from 50.5°C to 53.7°C. In the HW circulation are recorded temperature from 47.5°C to 50.8°C.

On uneven water temperatures mainly it affects the daily course of water consumption. Between 20.00 to 23.00 hours, where there is the biggest consumption of the hot water the HW temperature is the lowest and between 3.30 to 6.00 hours the temperature is highest. This is due to the fact that water is not taken from the system. In view of the fact that the mode of water consumption is different for each day, there is also a course of temperatures different.

When is no water consumption in the distribution system and only when hot water circulates in the system, it is possible to achieve a constant temperature at the installed temperature sensor. This situation is in practice unrealistic and even undesirable as distribution line should be used to distribute hot water to points of supply.

It follows the course of temperatures is possible to state that the removal hot water from the system is replaced in adequate quantity of cold water blended with storage water heaters, causing a change in water temperature in the system.

Since the amount of hot water removal from the system is non-uniform and is dependent on the human factor and also the performance of the water heater is designed for constant power, the water outlet temperature of the heater varies for each time point.

4.2 *Test measurements with continuous operation of the HW distribution system after distribution systems reconstruction*

The test measurement was carried out in June after reconstruction distribution of hot water and was carried out with continuous operation of the distribution system. The recording interval of the measured temperature was 30 minutes. Figures 5 and 6 show the weekly course of the measured temperatures of hot water and hot water circulation.

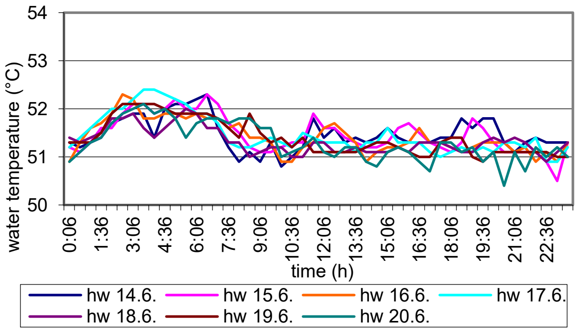

Figure 5 The course of the hot water temperature in insulated pipes

From Figures 5 and 6 it is clear that the temperature course of the heat-insulated tubes are on for less uneven than for non-insulated pipes.

In the pipeline are recorded hot water temperature from the 50.5°C to 52.5°C. In the hot water circulation pipeline are recorded temperature values from 46.1°C to 48.2°C.

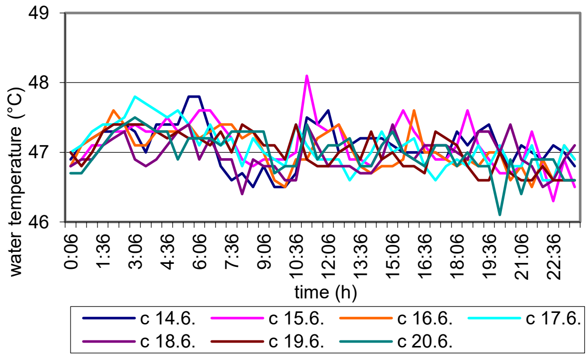

Figure 6 The course of the hot water temperature in insulated circulation pipes

5 Discussion

The total heat requirement to ensure supply of hot water in the flat consists of a heat demand for hot water delivered to the flat (heat consumed by the consumer) and the heat demand to provide hot water distribution (heat losses of hot water distribution pipes). For analyzed residential building is calculated specific and proportional heat consumption of the hot water supplied to the flat and the heat loss of hot water distribution. The specific heat consumption for heating of hot water supplied to the flat and specific heat loss of hot water distribution is shown in Figure 7.

The specific heat loss of hot water distribution with risers covered in felt belt (λ = 0.07 W.(m.K)$^{-1}$) 4 mm thickness is 7.11 GJ/flat per year. The specific heat loss of hot water distribution with risers with thermal insulation (λ = 0.04 W.(m.K)$^{-1}$) 20 mm thickness is 2.98 GJ/flat per year. The analysis considered the theoretical quantity of heat consumed to heat 1 m^3 of water from 10°C to 55°C with Q = 0.18738 GJ.m^{-3}.

From the graph in Figure 7, it is possible for any hot water consumption in the flat to determine what will be the percentage of heat consumed for the distribution of hot water and the percentage of heat consumed in the form of hot water supplied to the flat for insulated and non-insulated hot water risers.

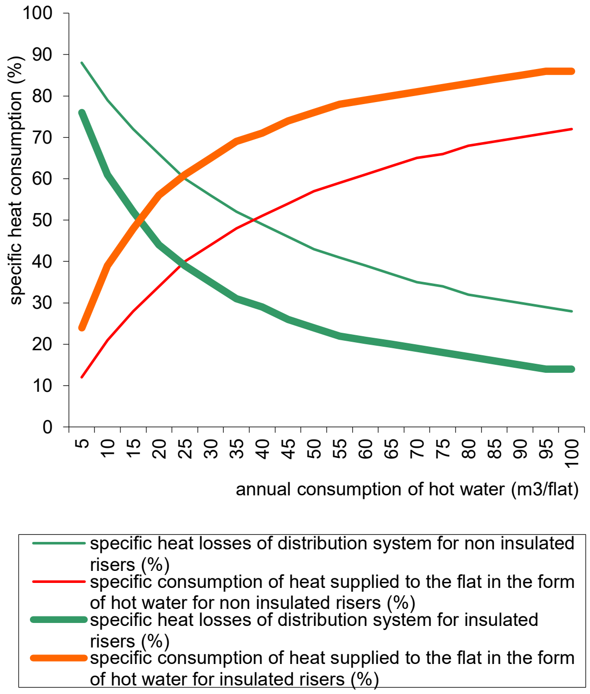

Figure 7 Specific consumption of heat supplied to the flat in the form of hot water and specific heat loss of hot water distribution system, depending on the annual consumption of hot water (%/flat)

For example, in residential buildings with a risers covered in felt belts, for an average flat with three inhabitants, with an annual consumption of hot water 60 m^3/flat is the total theoretical annual heat consumption Q = 18.33 GJ/flat. For that flat (Figure 7) it is 61% of the heat consumed for hot water supplied to the flat and 39 % of heat is lost as heat dissipates from the distribution pipeline.

After useing of thermal insulation for risers with a thickness of 20 mm ($\lambda = 0.04$ W.(m.K)$^{-1}$), the theoretical total annual heat consumption is Q = 14.20 GJ/flat. For that flat (Figure 7) will be 79 % of the heat consumed for hot water supplied to the flat and 21 % of heat will be lost as heat dissipates from the distribution pipeline.

After using of thermal insulation for risers in residential buildings can be theoretical heat consumption reduced at 75 % of the original heat consumption.

6 Conclusion

To ensure the comfort and hygienically clean hot water distributed in an apartment building it is necessary to provide the temperature of hot water in the range of 50 to 55 °C. It appears from the test measurements, that the temperature of the distributed hot water before isolating the pipes was in the range from 50 to 54°C and the hot water circulation pipes was in the range from 48°C to 51°C.

After isolating of the distribution pipes the temperature of hot water was in the range from 51°C to 52°C and in the hot water circulation pipes was the range of hot water from 46°C to 48°C. From experimental measurements it is possible to observe a decrease of the temperature in the distribution pipes by about 2°C, thus making it possible to achieve savings in energy, while ensuring comfort and hygiene and quality requirements for hot water.

7 The reference list

[1] KAPALO P., LUKÁČ P.: Temperature changes of hot water distribution system. *Journal of Applied Science in the Thermodynamics and Fluid Mechanics*. Vol. 4, No. 1, pp.1-5, 2010.

[2] STN EN ISO 12241: Thermal Insulation of Technical Equipment of Buildings and Industrial Installations - Calculation Rules, 2009.

[3] DECREE of the ME of the SR no. 282/2012 Col.of laws, establishing technical requirements for thermal insulation of heat and hot water distribution.

[4] HOLMAN J. P.: *Heat transfer - 8th ed.* New York, McGraw-Hill, 1997, 696 p.

Acknowledgement

This article was supported by the state grant agency for supporting research work and co-financing the project VEGA 1/0626/20.

Advances in Thermal Processes and Energy Transformation
Volume 5, 2022, POLI01, p. 45-54, ISSN 2585-9102
https://doi.org/10.54570/atpet

Experimental Devices for Measuring Small Gas Flows

Nikolas Polivka[1] ● Ján Kizek [1] ● Miroslav Rimár[1] ● Augustín Varga[2] ● Juraj Roth[2]

[1]Technical University of Košice, Faculty of Manufacturing Technologies with a seat in Prešov, Department of Process Technique, Bayerova 1, 080 01 Prešov, Slovak Republic, nikolas.polivka@tuke.sk, jan.kizek@tuke.sk, miroslav.rimar@tuke.sk
[2]Technical University of Košice, Faculty of Materials, Metallurgy and Recycling, Institute of Metallurgy, Letná 9, 042 00 Košice, Slovak Republic, augustin.varga@tuke.sk, juraj.roth@ptacek.sk
Category : Original Scientific Paper
Received : 15 October 2022 / Revised: 27 October 2022 / Accepted: 28 October 2022

Keywords: experimental device, gas flow, pressure loss,

Abstract: In this paper, the authors present the design of an experimental device for measuring small flow rates of gaseous media. For the design and construction, materials were used to create a local pressure resistance and thus allow the pressure gradient to be measured upstream and downstream of the measuring element. The proposed measuring devices can serve as an alternative to actual measuring devices for detecting the instantaneous quantity flowing in the measuring assembly. The results obtained from the experimental measurements are used to determine the characteristics of the proposed measuring elements. The aim is to establish dependencies that will serve for the use of the proposed measuring elements for research and educational purposes.

Citation: Polivka Nikolas, Kizek Ján, Rimár Miroslav, Varga Augustín, Roth Juraj: Experimental Devices for Measuring Small Gas Flows, Advance in Thermal Processes and Energy Transformation, Volume 5, No.3, (2022), p. 45-54, ISSN 2585-9102. https://doi.org/10.54570/atpet

1 Introduction

Flow meters of various designs are currently used for flow measurement, operating on the basis of different measurement principles. Basically, flow meters are divided into two groups based on the method used, namely volumetric and velocity flow meters [1,2]. Another criterion may be the physical principle of measurement, construction, type of fluid to be measured, etc. In some cases, it is not possible to determine clearly the exact method of flow measurement [1,3,4].

The volumetric method of measurement provides the possibility of defining an accurate volume in a bounded space. In contrast, the velocity method provides information on the instantaneous flow rate of a given fluid. Common to the determination of the flow rate for both methods is the need to know the properties of the flowing fluid, which can then be converted to normal conditions (0°C, 101325 Pa) or to commercial conditions that are agreed in a commercial relationship, e.g. as specified in [5].

Current measuring devices are manufactured according to customer or industry-specific requirements [6,7], the municipal sector or laboratories [8,9,10] or research purposes. It is important to measure the flow rates for immediate adjustment of the optimum parameters of a given process, such as for example in combustion of combustion air and fuel flow [9] or for overflows in cooling systems [11,12] or monitoring and diagnostics [13] of the monitored processes and processes.

There are specific calculations for the flow rate in the measuring device [1,3,4], based on which accurate flow rates for selected fluids can be determined. Experimentally determined conversion coefficients are used for this purpose, which have been obtained just by experimental measurements. The analysis of the obtained results was used to find the context for their further use or the suitability of the fluid for accurate flow measurement on the given measuring device.

The negative impact of losses due to improper selection and use of instruments can be largely avoided by understanding the physics involved in the instruments.

In the article, the authors proposed physical models for alternative measurements of low(small) flows. For the design and implementation of the experimental setup, the available materials were used, with the help of which the local pressure loss was generated. The principle of flow measurement is based on actual measuring devices such as measuring orifice [1,2,3, 13-16] or lamina flow elements [1], on which the differential pressure upstream and downstream of the measuring element is monitored. The flow rate is then recalculated according to the physical properties of the fluid to be measured [1,3,4,17].

2 Materials and methods

In designing the experimental setup, the authors based the design of the measuring element for monitoring the local pressure drop upstream and downstream of the measuring element based on relation (1) [17,18]:

$$\Delta p = \xi \frac{w_t^2}{2} * \rho_t \tag{1}$$

ξ - the calculated local pressure loss coefficient, (-),
Δp – pressure difference at the device, (Pa),
ρ_t– density of the flowing medium at the measured pressure and temperature, (kg.m^{-3})
w_t – the actual velocity of the fluid flow, at the measured pressure and temperature, (m.s^{-1}).

Calculation to zero conditions

A very important fact about the measured values is that the values obtained were measured at ambient temperature and barometric pressure at the time of measurement. For this reason, the measured values of the flow rates need to be recalculated.

The measured flow values at the flowmeter were converted to normal (0°C, 101325 Pa) using the relationship [17]:

$$q_{v0} = q_v \sqrt{\frac{T_0}{p_0}} \sqrt{\frac{p_1}{T_1}} \tag{2}$$

q_v- the actual flow rate measured at the flowmeter at the measured temperature t_1 and the measured pressure p_1, (l.h^{-1}),
q_{v0}- the calculated flow rate at the flowmeter at temperature t_0 and pressure p_0, (l.h^{-1}),
p_1- the actual total pressure at the inlet of the device, (Pa),
T_1- the actual inlet temperature to the measuring device, (K).

2.1 Measurement methodology

For the realization of the measurements, different circuits were used in order to be able to measure the produced models, for two different flow media, namely for air and natural gas (composition of natural gas from [5]).

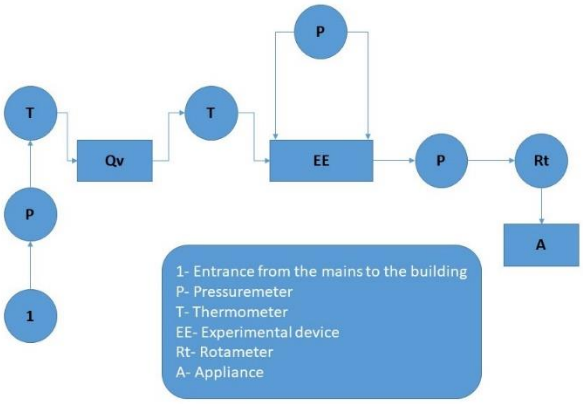

Figure 1 Schematic diagram of the measurement setup of the connection of the experimental device for measurement with air

For the calibration of the air flow equipment, a G4 BK type volumetric flowmeter was used, which had a value of the maximum permissible flow rate Q_{max} = 6 m^3.h^{-1} and the minimum flow value Q_{min} = 0.016 m^3.h^{-1}. The maximum input pressure that can be measured on this device is P_{max}= 20 kPa.

Figure 2 Volumetric flowmeter type G4 BK

Temperature and pressure readings were monitored at the inlet to the flow meter, which was connected downstream of the compressor. Downstream of the flowmeter, a fabricated experimental device was connected, at the inlet of which the temperature and pressure values of the flowing medium were measured. Just downstream of the device, the pressure at the end of the device was measured, from which the pressure difference at the beginning and end of the device was determined, i.e., the magnitude of the induced local pressure loss was determined. Downstream of the device, a float flow meter was connected to check that the maximum allowable flow rate on the device used for the calibration of the experimental device was not exceeded.

When comparing the errors of the measured flow rate on the volumetric flowmeter against the measured values on the rotameter, the highest error was 2 %. TESTO type pressure gauges with a measuring range of 2 - 20 kPa were used to measure the inlet pressure at the fabricated measuring device and to measure the pressure difference at the inlet and outlet of the device. For more accurate results, more precise measuring instruments could be used, which would guarantee a more accurate calibration of the experimental device. A Comet System MS3 type recording unit with a temperature measurement range of -70 to 1300°C and internal temperature compensation was used to measure both the inlet temperature of the volumetric flowmeter and the inlet temperature of the experimental device.

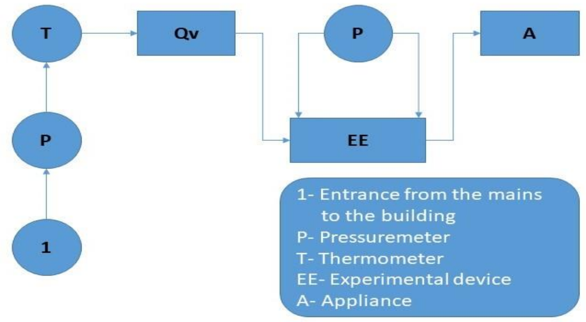

Figure 3 Schematic diagram of the measurement setup of the connection of the experimental device for measurement with natural gas

Using natural gas as the flowing material, a volumetric flow meter at the building inlet was used to calibrate the device and was used to measure the natural gas consumption in the laboratory building. The inlet pressure, inlet gas temperature and of course the flow rate were measured. This volumetric flowmeter was marked G40 BK. Maximum permissible flow rate Q_{max}= 65 m^3.h^{-1} and the minimum permissible flow at this flow meter is set at Q_{min}= 0.4 m^3.h^{-1}. The maximum input pressure that can be measured on this device is p_{max}= 10 kPa. Behind these devices was connected a fabricated experimental apparatus from which the natural gas was diverted to a burner on which this gas was burned. The natural gas measurements were made with pressures that were directly at the inlet of the pipeline. And since there was no device available to increase this inlet pressure to the plant, measurements were made only for the amount of gas present and the maximum pressure in the pipeline system. The pressure gauges used to measure the inlet pressure, at the manufactured device and to measure the pressure differential at the inlet and outlet of the device were digital from Testo with a maximum measured pressure of up to 200 kPa.

Figure 4 G40 BK volumetric flowmeter used in natural gas measurement

3 Physical models-experimental device

The authors focused in the paper on the design of 2 experimental devices, which are structurally different but with the same principle of determining the flow through the measuring element of the device. Physical models were designed for the same inlet and outlet pipes.

3.1 Experimental device No.1

The dimensions and schematic of the experimental setup No.1 are shown in the following figures.

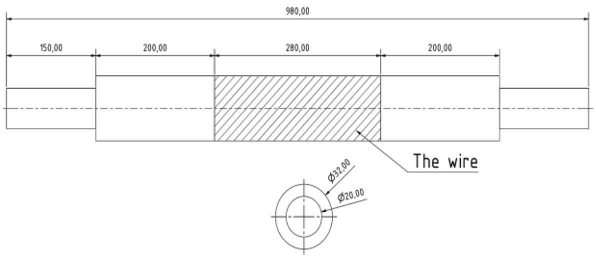

Figure 5 Drawing of model No.1

Experimental Device No.1 was fabricated using kitchen wire to simulate local pressure loss in the pipeline. A 32mm diameter waste pipe was used to fabricate the model. The total length of the pipe was 68cm, both before and after this pipe a 15cm length of PPR20 pipe was welded to provide the connection of the device to the instrumentation. At a distance of 45 cm from the start of the model (including the PPR20 pipe), kitchen wire weighing a total of 60g was placed behind the 32 mm diameter pipe. The wires are deposited over a length of 28 cm. Both just before and just after the deposited wires, M4 threaded holes were drilled for entry to the pressure gauges, which measured the static pressure at the start of the device and the pressure difference at the start and end of the device. To ensure the airtightness of the plant, all 'joints' and points where gas leaks could occur were secured with a fusion gun and silicone.

Figure 6 Inserting the wires into the measuring element

Figure 7 Finalization of the experimental device No.1

3.2 Experimental device No.2

The dimensions and schematic of the experimental device No.2 are shown in the following figures.

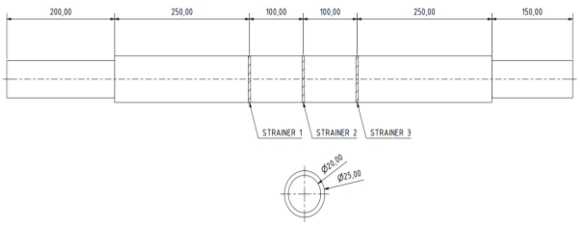

Figure 8 Schematic drawing of measuring element No.2

In the second model, siphon strainers were used to induce local pressure loss. The strainers were placed in the PPR25 pipe by placing three strainers in series with a 10cm spacing. Before the first strainer and just after the last strainer, holes were drilled with M4 threads, for pressure measurement on the pressure gauges. At the holes and measured the static pressure at the beginning and the difference (differential) of the pressures at the beginning and at the end of the measuring element.

The measuring element was modified so that before the first and after the last strainer, a PPR25 pipe with a length of 20 cm was welded. Subsequently, a pipe reduction to PPR20 was added at the inlet and outlet so that the compressor could be connected. The length of both PPR20 was 15 cm. The total length of the fabricated device was 90 cm. All "joints" were welded with a plastic pipe welder for this model.

Figure 9 Inserting the strainer into the measuring element

Each of the experimental devices was designed to generate a local pressure loss at the measuring element and, according to the pressure loss and the measured flow rate, individual dependencies were subsequently generated so that the flow rates of the media used could be determined from the pressure difference. The devices had different pipe diameters, lengths and locations of obstructions that created the pressure loss.

4 Results and discussion

Flow rate measurements using the available gaseous media were performed on the constructed experimental models for gaseous media flow measurements. The gaseous media used were air and natural gas from a low-pressure pipeline network (2.2 kPa). Based on the experimental measurements performed, the results obtained were processed and are presented in the following tables and graphs. The measurements were carried out according to the measurement schemes shown in Figure 1 and Figure 3.

4.1 Experimental device No.1 - Air

The flow rate measurements on the experimental device No.1 were carried out at an ambient temperature of 18.8°C and an atmospheric pressure of 100.8 kPa. The results from the measurements and the calculated flow rate values for air are shown in Table 1.

From the measured temperature of the air as a flow medium, it is possible to observe its increase due to the compression work performed by the fan used. Part of the compression work of the fan has been transformed in the form of a body which has been partially dissipated by the flowing air.

Table 1 Measured and calculated values - experimental device No.1 - Air

	Volume flowmeter				Experimental device				
	t_1 (°C)	p_1 (Pa)	q_v ($l.h^{-1}$)	q_{v0} ($l.h^{-1}$)	t_2 (°C)	p_2 (Pa)	Δp (Pa)	Re (-)	ξ
1	20.1	970	1780.53	1717.78	20.2	900	20	1430	83.61
2	20.1	1486	2677.82	2583.45	20.3	1300	510	2150	82.25
3	20.6	1916	3346.12	3228.20	20.6	1500	750	2680	77.73
4	21	1415	3940.04	3801.18	20.8	2000	1050	3160	78.75
5	21.7	1846	4442.31	4285.75	20.9	2300	1320	3560	78.14
6	22.3	3344	4920.19	4746.79	21.1	2800	1630	3950	78.93
7	23.2	3902	5418.73	5227.76	21.2	3300	1970	4350	78.91
8	24.2	4440	5879.14	5671.95	21.6	3800	2310	4720	78.87

t_1 – inlet temperature - flowmeter BK G4, (°C),
p_1 – inlet pressure - flowmeter BK G4, (Pa),
q_v – measured volumetric flow rate - flowmeter BK G4, ($l.h^{-1}$)
q_{v0} – volumetric flow rate (0°C, 101325 Pa), ($l.h^{-1}$),
t_2 – inlet temperature - experimental device. (°C)
p_2 – inlet static pressure - experimental device, (Pa)
Δp – pressure difference at the beginning and end of the measuring element, (Pa),
Re – calculated value of the Reynolds criterion [17], (-),
ξ - the calculated coefficient of local pressure loss, (-).

The coefficients ξ were expressed from relation (1) and recalculated for the actual flow rates and the diameter of the inlet pipe D to the measuring element.

$$\xi = \frac{2\,\Delta p}{w_t^2 \rho_t} = \frac{2\,\Delta p}{\left(\frac{4\,q_v}{\pi D^2}\right)^2 \rho_t} \tag{3}$$

In Figure 10, a graphical dependence is constructed for the calculated volumetric air flow rate q_{v0} and the pressure drop Δp at the measuring element.

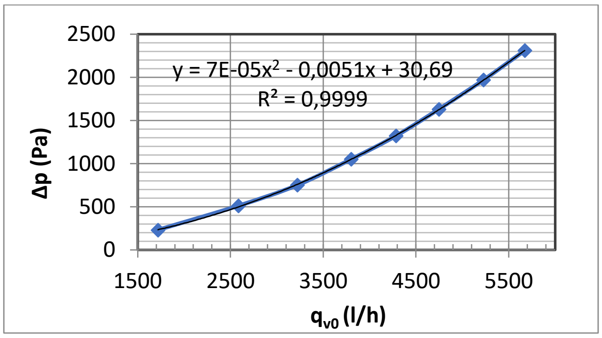

Figure 10 Dependence of the air flow rate on the change of the pressure difference at the measuring element – Air

The graphical dependence shows a quadratic increase of pressure loss with increasing amount of air flowing through the measuring element. The mathematical expression of the polynomial regression corresponds to this.

$$\Delta p = 30.69 - 0.0051\, q_{v0} + 7x10^{-5}\, q_{v0}^2 \tag{4}$$

In Figure 11 is constructed a graphical dependence of the calculated values of Re and the local pressure loss coefficient ξ on the measuring element. From the constructed dependence, a significant decrease of ξ can be observed, mainly in the laminar flow region. From this it can be concluded that the designed measuring element has a significant effect mainly in the laminar region and on the other hand in the transition region i.e. if Re>2300 ([17,18]) the coefficient ξ changes only minimally. Therefore, it can be concluded that at higher velocities, the coefficient ξ behaves as a constant value for the designed measuring element and the flow medium air. The correctness of the assumption would be confirmed by further measurements at higher air flow rates.

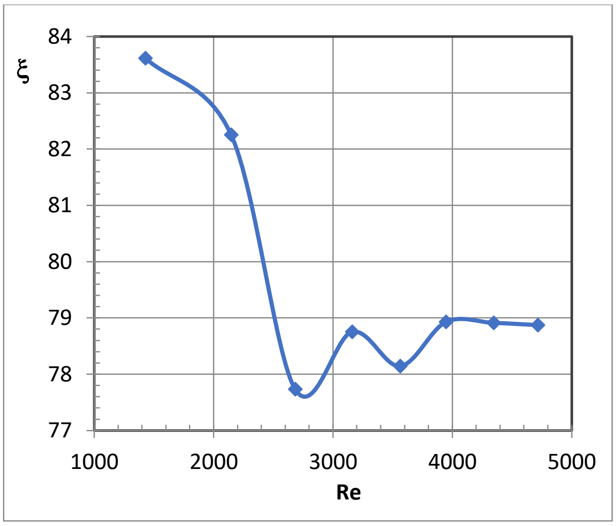

Figure 11 Dependence of the local pressure loss coefficient ξ on the calculated Re criterion – Air

4.2 *Experimental device No.1- Natural gas*

The measurement with natural gas was carried out under conditions of barometric pressure 102 kPa and ambient temperature 22°C. In the calculations, the temperature of the measured natural gas was considered as a constant value because there was no compression as with air and therefore the gas temperature did not increase. Since the pressure drop was made at low pressure, the effect of temperature change due to the Joule-Thomson effect in throttling of gases is not considered here either.

Table 2 Measured and calculated values - experimental device No.1- Natural gas.

	Volume flowmeter				Experimental device			
	t_1 (°C)	p_1 (Pa)	q_v ($l.h^{-1}$)	q_{v0} ($l.h^{-1}$)	p_2 (Pa)	Δp (Pa)	Re (-)	ξ
1	15	1920	841.39	812.12	400	80	576	218.62
2	15	1960	1179.09	1138.07	700	10	807	166.99
3	15	1980	1343.94	1297.18	900	140	920	149.96
4	15	1980	1527.72	1474.57	1300	180	1050	149.21
5	15	2000	190.05	1840.70	1800	240	1300	127.67

t_1 – inlet gas temperature from the pipeline, (°C),
p_1 - inlet gas pressure from the pipeline, (Pa),
q_v – measured volumetric flow rate - flowmeter BK G4, ($l.h^{-1}$)
q_{v0} – volumetric flow rate (0°C, 101325 Pa), ($l.h^{-1}$),
p_2 – inlet static pressure - experimental device, (Pa)
Δp – pressure difference at the beginning and end of the measuring element, (Pa),
Re – calculated value of the Reynolds criterion [17], (-),
ξ - the calculated coefficient of local pressure loss, (-).

From the calculated values of Re it can be concluded that the flow measurement on the experimental device up to the maximum overpressure from the gas pipeline of 2 kPa, the flow is located only in the laminar regime [17] region of the gas flow in the inlet pipeline.

By not using a float flowmeter (rotameter) for the gas measurement due to the large pressure loss, it was possible to recalculate the measured flow on the volumetric flowmeter and no measurement error was considered when the rotameter was switched on.

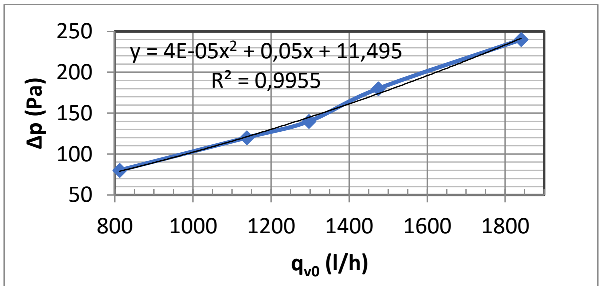

Figure 12 Dependence of the flow rate on the pressure differential across the measuring element -Natural gas

Similar to the air measurement, the regression analysis can be used to determine the quadratically increasing trend of the pressure gradient change at the measuring element as the natural gas flow rate increases.

$$\Delta p = 11.495 + 0.05\, q_{v0} + 4x10^{-5}\, q_{v0}^2 \qquad (5)$$

From these measured and calculated values, a dependency was then made. The ξ coefficients were obtained after modifying the relation (1) and calculated by the relation (3).The gas density was taken from the available literature [5] and its value was 0.717 kg/m^3.

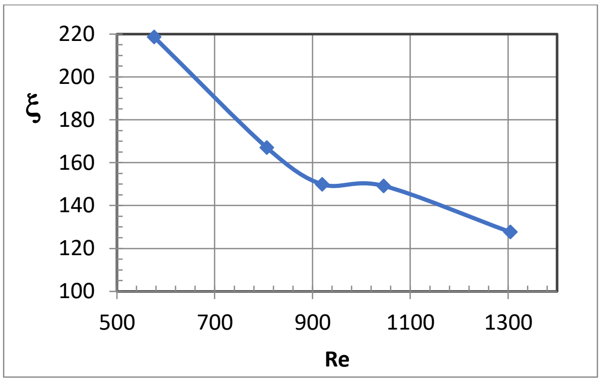

Figure 13 Dependence of the local pressure loss coefficient ξ from the calculated Re criterion – Natural gas.

In Figure 13 it is possible to observe from the constructed graphical dependence the decreasing trend of the coefficient ξ depending on the increasing velocity of the gas through the measuring device. A decreasing trend also occurred for air in the laminar flow region. Therefore, a similar trend in the local pressure loss coefficient ξ can be assumed for each gaseous medium. This statement can be verified using other gaseous media.

4.3 Experimental device No.2- Air

Unlike the first model, the No.2 device is constructed as a set of multiple identical obstacles that cause a gradual pressure drop. Siphon strainers were used as the local resistance, which are typed and thus the pressure drop characteristic can be determined even for a single element. The measured and calculated results obtained are presented in the following tables and graphs.

The measurement with air was carried out at a barometric pressure of 100.7 kPa and an ambient temperature of 19.2°C.

Table 3 Measured and calculated values - experimental device No.2- Air

	Volume flowmeter				Experimental device				
	t_1 (°C)	p_1 (Pa)	q_v $(l.h^{-1})$	q_{v0} $(l.h^{-1})$	t_2 (°C)	p_2 (Pa)	Δp (Pa)	Re (-)	ξ
1	23.3	1046	1881.23	1812.79	21.7	700	260	1930	31.73
2	23.7	1721	2709.65	2611.07	21.7	1100	570	2780	33.52
3	24.3	1995	3315.42	3194.80	21.8	1600	900	3400	35.48
4	24.5	2445	3820.03	3681.05	21.7	2000	1210	3920	36.05
5	24.7	1964	4282.31	4126.52	21.4	2600	1580	4390	37.59
6	24.2	3482	4743.74	4571.16	21.3	3100	1980	4860	38.51
7	23.1	3991	5185.53	4996.88	20.8	3700	2400	5320	39.20

t_1 – inlet temperature - flowmeter BK G4, (°C),
p_1 – inlet pressure - flowmeter BK G4, (Pa),
q_v – measured volumetric flow rate - flowmeter BK G4, $(l.h^{-1})$
q_{v0} – volumetric flow rate (0°C, 101325 Pa), $(l.h^{-1})$,
t_2 – inlet temperature - experimental device. (°C)
p_2 – inlet static pressure - experimental device, (Pa)
Δp – pressure difference at the beginning and end of the measuring element, (Pa),
Re – calculated value of Reynolds criterion [17], (-),
ξ - calculated coefficient of local pressure loss, (-).

From the calculated flow rates to normal conditions according to (2), the dependence of the pressure drop at the measuring device on the air flow rate was constructed, which is shown in Figure 14.

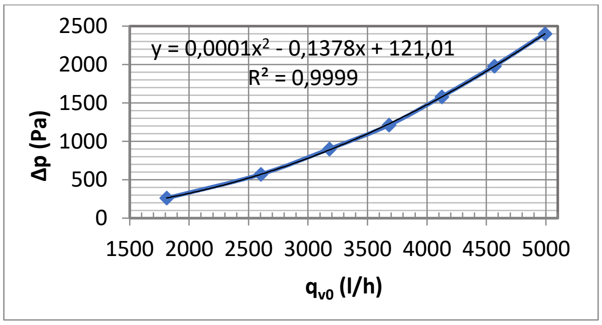

Figure 14 Dependence of the pressure drop across the device as a function of the normal flow rate - Air

After the addition of the trend regression curve, the pattern of the increase in pressure change can again be described by a quadratic equation, which can be written as:

$$\Delta p = 121.01 - 0.1378\, q_{v0} + 1x10^{-4}\, q_{v0}^2 \qquad (6)$$

Similar trend dependencies could be expected when using one element or even more than 3 elements. For a given range of flow rates, the pressure gradient would increase as the number of elements inserted increases.

As with the first measurement, this measurement recalculated the coefficients for each row of the table. From these measured and calculated values, a dependency was then made. The local pressure loss coefficients were calculated according to the relationship (3).

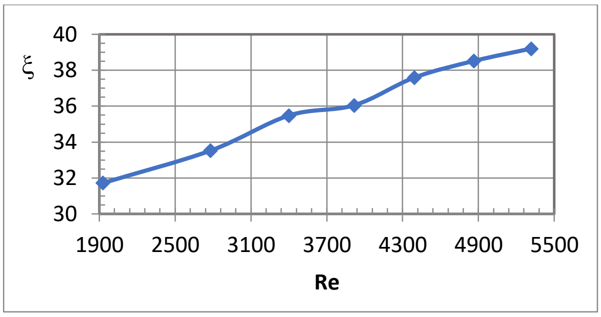

Figure 15 Dependence of the coefficient ξ on the calculated Re criterion – Air.

From Figure 15, an increase in the local pressure loss, or 3 inserted elements (strainers), can be observed. According to [17,18], the given dependence is evaluated as the sum of the coefficients ξ in a given gauge system. Since each strainer represents a separate local pressure loss.

4.4 Experimental device No.2- Natural gas

The measurement with natural gas was carried out at a barometric pressure of 102 kPa and an ambient temperature of 22°C. The density of natural gas was taken from the available literature [5] and its value was 0,717 kg.m^{-3}.

In the measurement, as in the case of the measurement on measuring device No.1, a constant temperature of the natural gas was considered due to the omission of the compression device, which by its work increased the air temperature.

Table 4 Measured and calculated values - experimental device No.2- Natural gas

	Volume flowmeter				Experimental device			
	t_1 (°C)	p_1 (Pa)	q_v (l.h^{-1})	q_{v0} (l.h^{-1})	p_2 (Pa)	Δp (Pa)	Re (-)	ξ
1	15	1950	1066.96	1029.84	500	30	934	18.99
2	15	1950	1373.23	1325.45	1000	70	1200	26.75
3	15	1980	1625.12	1568.58	1200	110	1420	30.02
4	15	1950	1690.19	1631.39	1400	130	1480	32.80
5	15	1950	1824.73	1761.24	1600	160	1600	34.63
6	15	1950	1916.79	1850.11	1800	190	1680	37.27

t_1 – inlet gas temperature from the pipeline, (°C),
p_1 - inlet gas pressure from the pipeline, (Pa),
q_v – measured volumetric flow rate - flowmeter BK G4, (l.h^{-1})
q_{v0} – volumetric flow rate (0°C, 101325 Pa), (l.h^{-1}),
p_2 – inlet static pressure - experimental device, (Pa)
Δp – pressure difference at the beginning and end of the measuring element, (Pa),
Re – calculated value of the Reynolds criterion [17], (-),
ξ - the calculated coefficient of local pressure loss, (-).

As with air, so with gas, measurements were taken at different conditions than the zero conditions. Therefore, it was necessary to convert the obtained flow rates to normal conditions. Since a float flowmeter was not used for the gas measurement, it is sufficient to convert the measured flow rate directly on the volumetric flowmeter using the relation (2).

In Figure 16, a graphical dependence of the pressure drop across the device as a function of the natural gas flow rate is constructed, which is converted to normal conditions according to (2). From the graphical representation, it can again be observed a quadratic increase in pressure gradient as a function of the increase in flow rate through the device.

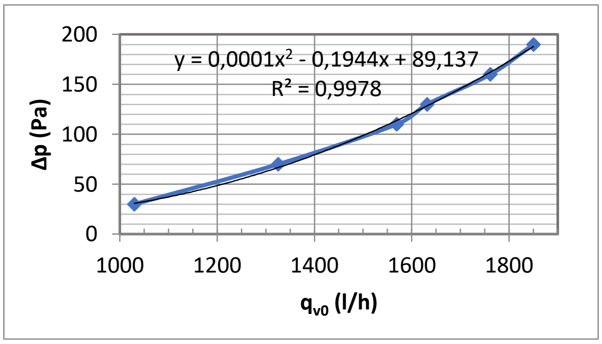

Figure 16 Dependence of the change in pressure differential across the device on the flow rate –Natural gas

After adding a trend regression curve, the pattern of the increase in the magnitude of the pressure drop can again be described by a quadratic equation, which can be written as:

$$\Delta p = 89.137 - 0.1944\, q_{v0} + 1x10^{-4}\, q_{v0}^2 \qquad (7)$$

The quadratic trend dependencies correspond to relation (1), where the pressure change is proportional to the square of the velocity.

Figure 17 shows a graphical plot of the local pressure loss coefficient versus increasing Re criterion or increasing flow through the measuring device.

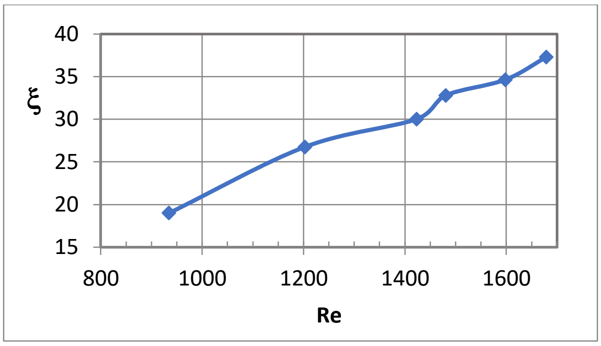

Figure 17 Dependence of the coefficient ξ on the calculated Re criterion – Natural gas

The graphical dependence of the coefficient ξ is also increasing in the case of natural gas. In contrast to model No.1, the proposed device No.2 shows different characteristics in the observed flow rate range of the gaseous media used.

The proposed devices showed the possibilities for further investigation or design of similar devices or combinations of individual elements.

5 Conclusion

Among the advantages of the designed measuring elements (experimental devices), one could include low cost of production, theoretically achievable high accuracy with proper calibration, simplicity of construction, which is theoretically closely related to the low cost of maintenance and operation of these devices. Another advantage is that the flow rate is directly determined at zero (normal) conditions.

The disadvantages of these devices are the need to induce a certain pressure loss on the pipeline through which the gaseous medium flows and the need for additional measuring devices (pressure gauges, thermometers).

For experimental device No.1, it would be necessary to induce a greater pressure loss by using a larger number of wire tubes or to increase the density of the wire filler because at low flow rates (especially when measured using natural gas) the pressure difference across the device was relatively small, resulting in a higher inaccuracy of the device in measuring the flow. The density of the wirefill and the method of placement in the measuring element is limiting if the same measuring element needs to be manufactured. A new calibration and thus a new measurement characteristic for the newly created element is needed.

For experimental setup number 2, it would be advisable to design the metering element system so that the strainers can be selected and stacked in number as needed according to the predicted flow rates. By such a modification, the device could be used at both higher and lower flow rates, and by developing a greater resistance, theoretically a higher accuracy of the meter could be achieved.

Because of the commercially produced strainers and the assumption of equal pressure loss per strainer, the No.2 measuring element is more useful in the next design of measuring assemblies. Another advantage is the use in case of the need for a larger number of measured streams in a local measurement system.

The aim of creating a simple measuring element gives, on the basis of the measurements made, the possibility of further investigation or creation of new measuring elements of a different design.

6 The reference list

[1] MIKAN, J.: *Gas measurement*. Říčany u Prahy: GAS s.r.o., 2003.

[2] HALAJ, M., KUREKOVÁ, E.: Measurement of flow rate, overflow quantity (1), *AT&P journal, Princípy automatizácie*, No.11, pp. 18-19, 2011.

[3] RAJNIAK, I., ZAVODNOV, P., KUČÁK, Ľ.: *Measurement in thermal power engineering*, Bratislava, ALFA, 1989.

[4] NUTIL, J., ČECH, V.: *Measurement in the metallurgical industry*, Praha, SNTL,1982.

[5] SPP-Distribucia: Natural gas composition and emission factor, [Online], Available: https://www.spp-distribucia.sk/dodavatelia/informacie/zlozenie-zemneho-plynu-a-emisny-faktor/ [20 Dec 2021], 2021.

[6] KREHEĽ, R., STRAKA, Ľ., KRENICKÝ, T.: Diagnostics of production systems operation based on thermal processes evaluation, *Applied Mechanics and Materials*, Vol. 308, pp. 121-126, 2013.

[7] KUZNETSOV, E., NAHORNYI, V., KRENICKÝ, T.: Gas Flow Simulation in the Working Gap of Impulse Gas-Barrier Face Seal. *Management systems in production engineering*, Vol. 28, No. 4, pp. 298-303, 2020.

[8] DURDAN, M., STEHLIKOVA, B., PASTOR, M., KACUR, J., LACIAK, M., FLEGNER, P.: Research of annealing process in laboratory conditions, *Measurement*, Vol. 73, pp. 607-618, 2015.

[9] HOLUBČÍK, M., ĎURČANSKÝ, P., NEMEC, P.: *The effect of the amount of combustion air to the furnace performance and emissions parameters*, Energy and clean technologies conference proceedings, SGEM 2016, International Multidisciplinary Scientific GeoConference-SGEM, Albena, Bulgaria, Vol. I., pp. 725-729, 2016.

[10] VILAGI, F., KNIZAT, B., MLKVIK, M., URBAN, F., OLSIAK, R., MLYNAR, P.: Mathematical model of steady flow in a helium loop, *Mechanics & Industry*, Vol. 20, No. 7, 704, 2019.

[11] RIMAR, M., FEDAK, M., KULIKOV, A., KRENICKY, T., KULIKOVA, O.: Influence of heat accumulation of the object on the operation of the cooled ceilings cooling system, *MM Science Journal*, No. 10, pp. 5931-5936, 2022.

[12] ĎAĎO, S. a kol. 2005. *Measurement of flow and height*, 3rd ed., Praha, Technical Literature BEN, 2005.

[13] KRÁLIKOVÁ R.: *Monitoring a diagnostika životného prostredia*, Košice, Technical University, 1999, pp. 108 -121.

[14] HALAJ, M., KUREKOVÁ, E.: Measurement of flow rate, overflow quantity (4). *AT&P journal, Princípy automatizácie*, No. 2, pp. 51-53, 2012.

[15] HALAJ, M., KUREKOVÁ, E.: Measurement of flow rate, overflow quantity (5), *AT&P journal, Princípy automatizácie*, No. 3, pp. 44 – 46, 2012.

[16] HALAJ, M., KUREKOVÁ, E.: Measurement of flow rate, overflow quantity (8), *AT&P journal, Princípy automatizácie*, No. 6, pp. 43-45, 2012.

[17] VARGA, A., JABLONSKÝ, G., LUKÁČ, L. KIZEK, J.: *Thermal technology for metallurgists* (In Slovak), 1.ed., Technical University in Košice, 2013.

[18] SVINOLOBOV, N.P., BROVKIN, V.L.: *Theoretical foundations of metallurgical heat technology*, Dnipro, Porogi, 2002.

Acknowledgement

This article was supported by the state grant agency for supporting research work and co-financing the project KEGA 023TUKE-4/2021.